Extracellular

Intracellular

β₂AR H8 pos. R333C   β₂AR TM6 pos. 265C   CB₁ TM6 pos. A342C   Opsin H8, pos. 316C
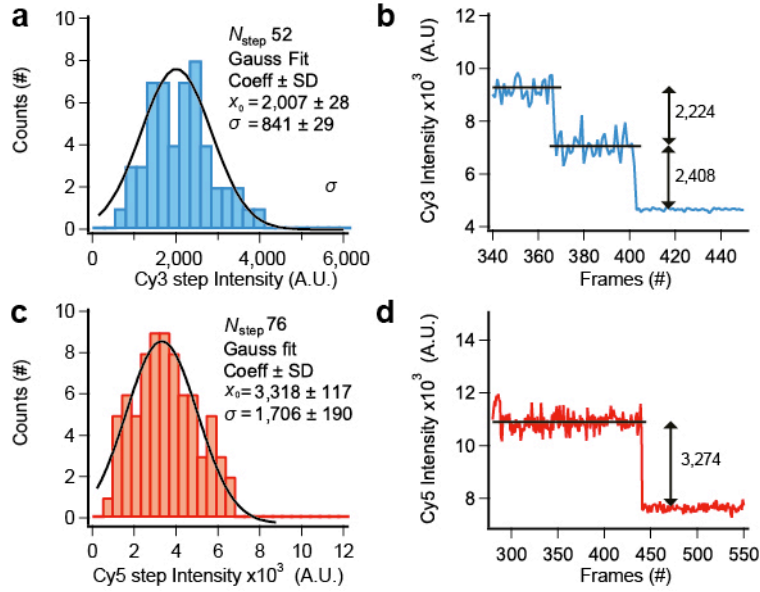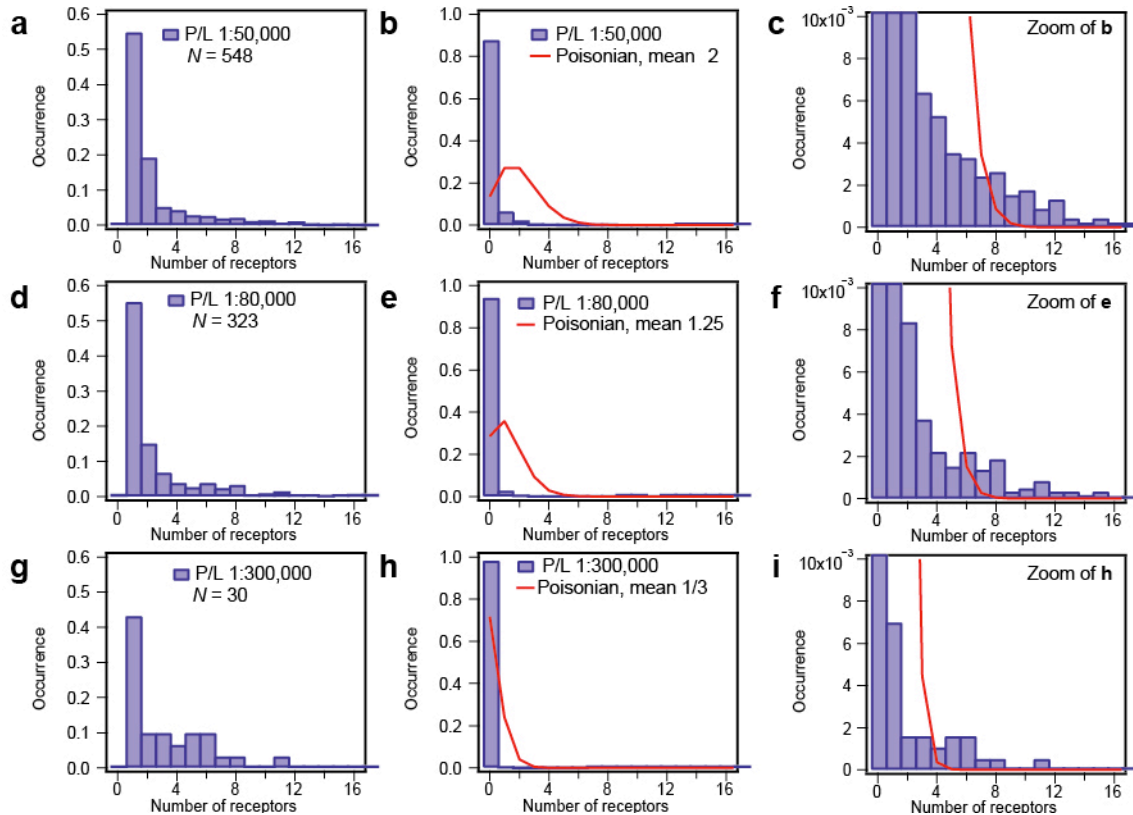
Supplementary Figure 1

GPCR labeling positions.

Positions of fluorescently labeled cysteines (marked by red) in the protein constructs employed in this study. β₂AR pdb code 2RH1. Currently no crystal structure is available for the CB₁, we therefore used a homology model based on pdb code 3V2Y, for illustrating the labeling position. Opsin pdb code 3CAP.

Supplementary Figure 2

Representative single-molecule bleaching steps for quantification of protein densities.

Single molecule bleaching steps was used as a calibration to determine the actual number of receptors on single proteoliposomes (see **online methods**). The most probable number of receptors was ~20 for the nominal P/L 1:1,000 shown in Fig. 2c. (**a**) A histogram of Cy3 single molecule bleaching step fitted with a gaussian. The peak position (x_0) of 2007 ± 28 is used for further analysis. (**b**) Example of Cy3 bleaching step. (**c**) A histogram of Cy5 single molecule bleaching step intensities fitted with a gaussian. The peak position (x_0) of 3318 ± 117 is used for further analysis. (**d**) Example of Cy5 bleaching step.

Supplementary Figure 3

Distributions of number of proteins for three of the different reconstitutions shown in **Figure 2b** (nominal P/L = 1:50,000, 1:80,000 or 1:300,000).

(**a-i**) The number of proteins was determined by single molecule photobleaching (**online methods**) for each individual reconstitution. (**a**) Distribution of number of proteins for nominal P/L 1:50,000. (**b**) Empty liposomes are included in the distribution of number of proteins for nominal P/L 1:50,000. In the case that insertion of receptors into the proteoliposomes is entirely random, the number distribution of receptors should be poissonian. A mean proteoliposome diameter of 100 nm corresponds to ~100,000 lipids pr. proteoliposome (using lipid headgroup area of 0.67 nm^2). For a reconstitution of 1:50,000 nominal P/L a poissonian distribution should therefore have a mean of 2 proteins pr. liposome. This distribution is plotted in red. (**c**) Zoom of **b**. (**d**) Distributions of number of proteins for nominal P/L 1:80,000. (**e**) Empty liposomes are included in the distribution of number of proteins for nominal P/L 1:80,000. (red) poissonian distribution for a mean of 1.25 proteins pr. liposome (assuming a mean number of lipids of 100,000 pr. proteoliposome). (**f**) Zoom of **e**. (**h**) Distributions of number of proteins for nominal P/L 1:300,000. (**i**) Empty liposomes are included in the distribution of number of proteins for P/L nominal 1:300,000. (red) poissonian distribution for a mean of 0.33 proteins pr. liposome (assuming a mean number of lipids of 100,000). (**j**) Zoom of **i**.
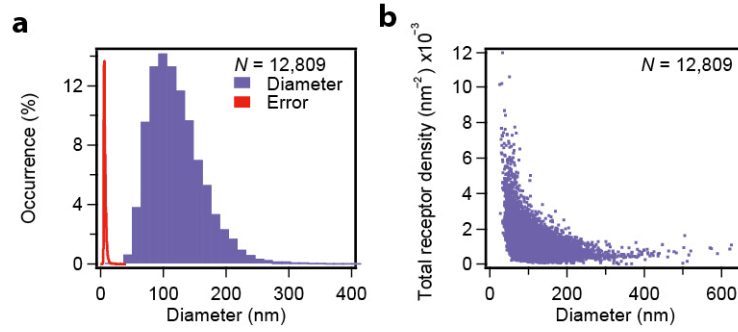
Supplementary Figure 4

Distribution of proteoliposome diameters and receptor density versus proteoliposome diameter, as found for β₂-AR (Δ5-R333C, nominal P/L = 1:1,000).

**(a)** Histogram of proteoliposome diameters. **(b)** Receptor density plotted against proteoliposome diameter.
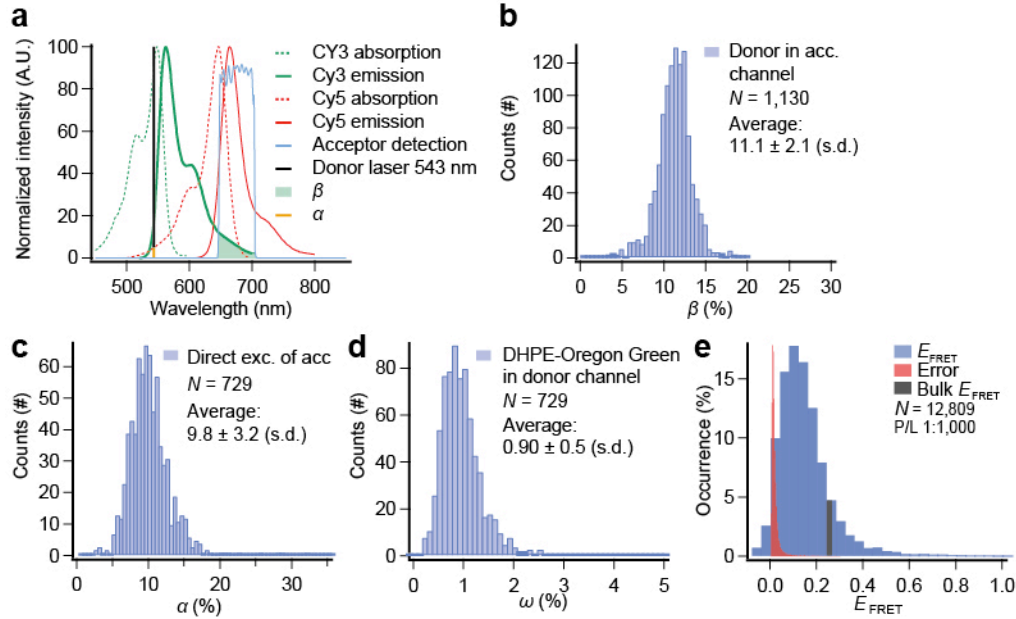
Supplementary Figure 5

Quantification of FRET correction factors.

(**a**) Cy3 (green) and Cy5 (red) absorption and emission spectra is shown together with donor excitation (543 nm, black vertical line) and acceptor emission bandpass filter (blue). Orange marks the direct excitation of acceptor by donor excitation 543 nm (α). Light green area marks the donor intensity in Cy5 detection channel β. (**b**) Histogram of the percentage donor intensity in acceptor channel at donor excitation (exc. 543 nm), β. β was calculated as the ratio of donor signal arising in the acceptor channel (exc. 543 nm) to the donor signal in the donor channel (exc. 543 nm). β was determined for 1,130 single proteoliposomes carrying only β_2AR-Cy3 (nominal P/L 1:1,000). (**c**) Histogram of percentage direct excitation of acceptor at donor excitation (exc. 543 nm), α. α was calculated as the ratio of acceptor signal (exc. 543 nm) in the acceptor channel to the signal of the acceptor excited at 633 nm. α was determined for 729 single proteoliposomes carrying only β_2AR-Cy5 (nominal P/L 1:1,000). (**d**) Histogram of the percentage Oregon Green-DHPE in donor channel at donor excitation (exc. 543 nm), ω. ω was calculated as the ratio of Oregon Green-DHPE intensity (exc. 543 nm) in the donor channel to Oregon Green-DHPE excited at 476 nm. ω was determined for 729 single liposomes carrying only Oregon Green-DHPE. (**e**) Histogram of single proteoliposome E_{FRET} (blue) and corresponding histogram of E_{FRET} errors (red) (β_2AR nominal P/L 1:1,000). The calculated ensemble average FRET efficiency $E_{FRET,bulk}$ is marked by the dark gray line.
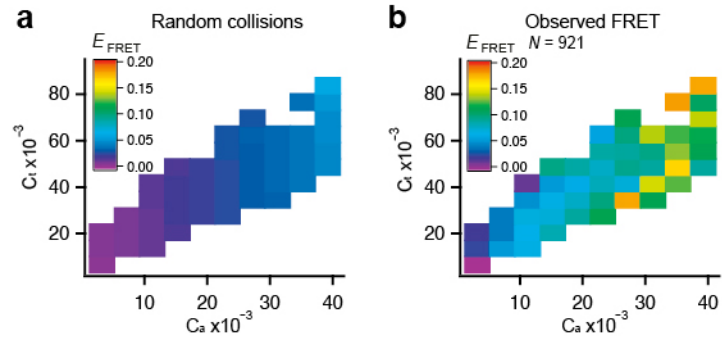
Supplementary Figure 6

Comparing the measured FRET efficiencies with FRET arising from random collisions.

(**a**) The predicted FRET efficiency of random collisions (colorscale) as accessed by eq. 7 in **Supplementary Note** for the range of reduced acceptor densities C_a and reduced total den. C_t measured in a single reconstitution sample (β_2AR, P/L 1:1,000). (**b**) For comparison the measured E_{FRET} (colorscale). The measured E_{FRET} is well above random collisions, and supports that we observe significant oligomerization.
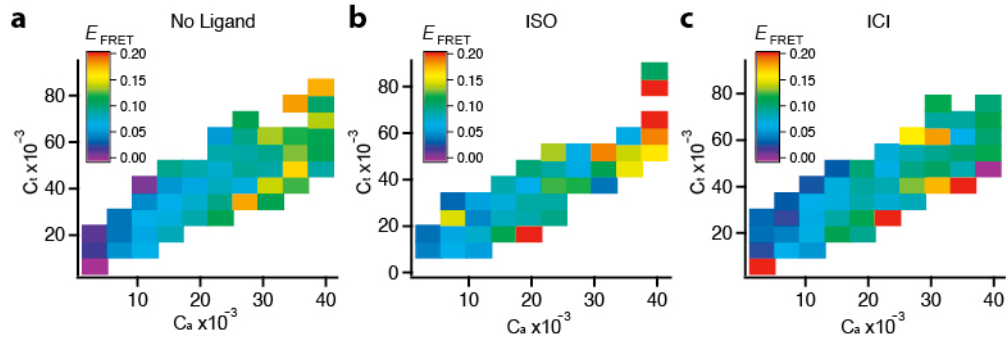
Supplementary Figure 7

The effect of ligands on β_2-AR oligomerization.

(a-c) Reduced total receptor density C_t and reduced acceptor density C_a as a function of E_{FRET} (color scale) for a population of proteoliposomes with a narrow size distribution of 120-130 nm. For better visualization E_{FRET} values of single liposomes in **a-c** are binned and a weighed average of each bin is shown. **(a)** No ligand treatment, N = 921 proteoliposomes. **(b)** Proteoliposomes incubated with saturating amounts (10 μM) of agonist Isoproterenol (ISO), N = 321 proteoliposomes. **(c)** Proteoliposomes incubated with saturating amounts (500 nM) of inverse agonist ICI 118,551 (ICI). N = 510 proteoliposomes.
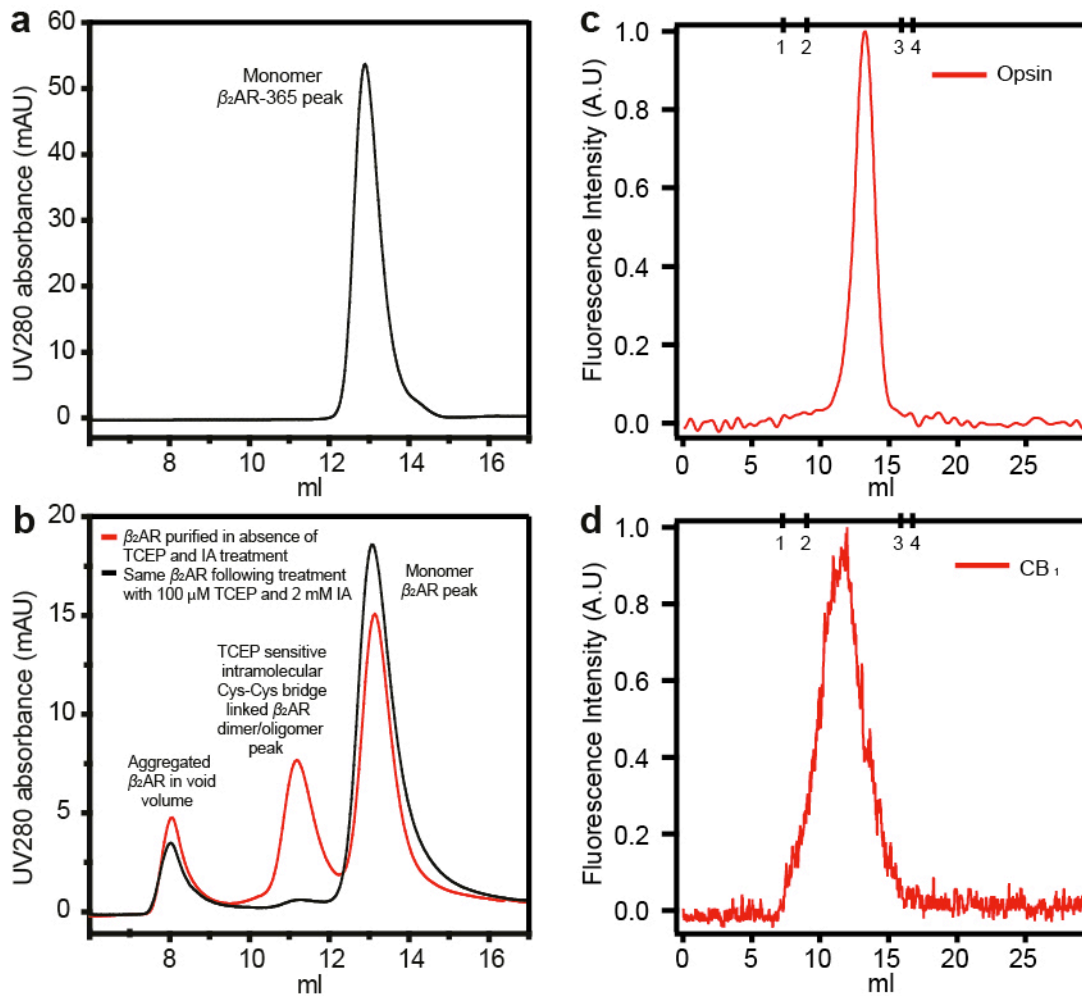
Supplementary Figure 8

GPCR size-exclusion chromatography elution profiles.

(**a**) Size exclusion chromatography (SEC) trace of detergent solubilized β_2AR-365 functionally purified by sequential antibody and ligand affinity chromatography. (**b**) Full-length β_2AR was functionally purified in absence of reducing reagent *tris*(2-carboxyethyl)phosphine (TCEP) and iodoacetamide (IA) allowing cysteine bridge formation between receptors. Size exclusion chromatography of the purified β_2AR was performed in absence (red) and following (black) of TCEP/IA pretreatment. In reducing conditions the fraction of monomeric detergent solubilized receptors increase and the dimeric/oligomeric species decrease. (**c-d**) Fluorescence-detected size-exclusion chromatography (FSEC) traces of purified Cy5 labeled detergent solubilized CB$_1$ and Opsin. About 25 pmoles of sample was injected into a 100 uL loading loop and then run over a hand packed 60 mL (34cm x 1.5 cm diameter) Superdex 200 (prep grade) column using 20 mM TRIS pH 7.5, 150 mM NaCl, 1mM EDTA and 0.05% DM at a flow rate of 0.5 mL/min. The elutions were monitored via a RF-551 fluorescence HPLC monitor (Shimadzu) with excitation wavelength set at 635 nm and emission wavelength set at 665 nm for Cy5. Elution time correspond to ~85 kDa for opsin and ~175 kDa for CB$_1$ as estimated from the their molecular weights (38.5 kDa and ~40 kDa) and the addition of a DM micelle. The markers: 1, 2, 3, & 4 represent molecular weight standards (void volume, 669 kDa, 43 kDa, and 27 kDa, respectively).
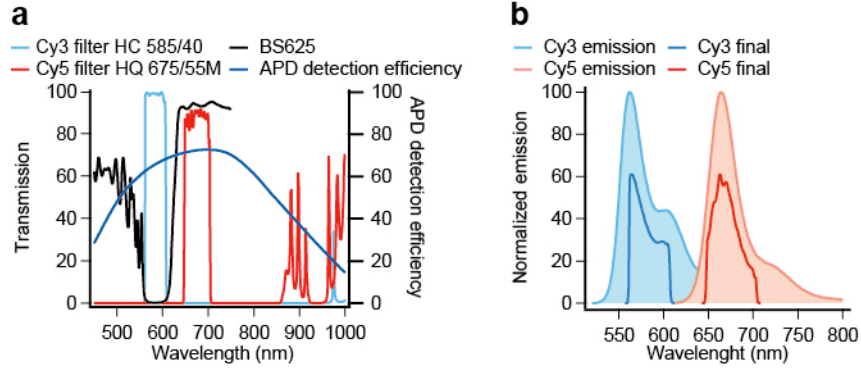
Supplementary Figure 9

Theoretical determination of (η_A/η_D).

(**a**) Transmission efficiency (left) for Cy3 bandpass filter (HC585/40), Cy5 filter HQ675/55M, and beamsplitter BS625. Detection efficiency for the APD (right) of type SPCM-AQR-13-FCM, Perkin Elmer. (**b**) Initial and final Cy3 and Cy5 emission spectra. Normalized Cy3 and Cy5 emission spectra and the reduced final emission after passing through each element in the optical pathway 1) beamsplitter 2) filter 3) APD, shown in **a**.

Supplementary Note

Theory for extracting protein-protein association energy

We selected a uniform size population for extracting the association equilibrium constant for β2AR to exclude the indirect contribution of membrane curvature to protein diffusion and thus to oligomerization[1]. As seen from **Supplementary Fig. 4b** the greatest density variations occur at proteoliposome diameters below 200 nm, we thus investigated the narrow range between 120-130 nm, which still provided a population of 921 single proteoliposomes.

The FRET efficiency for a random distribution of donors and acceptors in a two dimensional membrane was described theoretically by Wolber and Hudson[2]. The theoretical solution was solved numerically, and an analytical approximation is given by

Eq. 7 $$E_{random} = 1 - (A_1 e^{-k_1 C_a} + A_2 e^{-k_2 C_a})$$

Here the concept of reduced acceptor density C_a is introduced as the acceptor surface density multiplied by a Förster area (Förster radius R_0^2) (For Cy3/Cy5 R_0 =53 Å (ref. 3). $A_{1,2}$ and $k_{1,2}$ are constants that vary for different values of (R_e / R_0), R_e being the closest approach between donor and acceptor. Based on structural information R_e / R_0 was assumed to be 1 (ref. 4) for reconstituted β2AR.

For a system including dimerized donors and acceptors, the FRET efficiency is given by

Eq. 8 $$E_{FRET} = (1 - f_b) E_{random} + f_b E_{bound}$$

Where E_{bound} is the FRET efficiency within a dimer. E_{bound} is weighted by the fraction of bound donors f_b, which is also the probability that a randomly chosen donor is bound to an acceptor. f_b can be expressed as the probability that a single randomly chosen donor will be in a dimer f_d multiplied by the probability that the second unit in the dimer is an acceptor P_A (ref. 5).

Eq. 9 $$E_{FRET} = (1 - f_d P_A)E_{random} + f_d P_A E_{bound}$$

P_A is given by the acceptor molefraction, here expressed in terms reduced densities, C_a (reduced acceptor density), C_d (reduced donor density) and $C_t = C_a + C_d$ (reduced total receptor density)

Eq. 10 $$P_A = \frac{C_a}{C_a + C_d} = \frac{C_a}{C_t}$$

Combining eq. 7, 9 and 10, E_{FRET} is given by

$$E_{FRET} = \left(1 - f_d \frac{C_a}{C_t}\right)\left(1 - \left(A_1 e^{-k_1 C_a} + A_2 e^{-k_2 C_a}\right)\right) + f_d \frac{C_a}{C_t}E_{bound}$$

Eq. 11

For a monomer dimer equilibrium, $[M] + [M] \rightleftarrows [D]$, the association constant K_a and the standard Gibbs free energy change ΔG_a is given by

Eq. 12 $K_a = \dfrac{[D]}{[M]^2}$

Eq. 13 $\Delta G_a = -RT\ln(K_a)$

2

As pointed out by Fleming *et al.*[6] it is crucial for a correct thermodynamic description of protein association in a hydrophobic solute to apply the effective concentration of proteins in the lipid phase. This is in contrast to, for example, protein concentration in the total volume of buffer and lipids. In accordance with this we employed the mole fraction scale, permitting extraction of a standard Gibbs free energy that can be directly compared to reported literature values.

The fraction of dimers can be expressed in terms of K_a and the total receptor mole fraction X_p according to eq. 14 (ref. 7)

Eq. 14
$$f_d = \frac{4K_aX_p + 1 - \sqrt{8K_aX_p + 1}}{4K_aX_p}$$

Where X_p is given by

Eq. 15
$$X_P = \frac{2N_{protein}}{2N_{protein} + N_{lipids}} = \frac{2N_{protein}}{2N_{protein} + 2\dfrac{A_{liposome}}{A_{lipid}}}$$

$N_{protein}$ and N_{lipids} being the numbers of receptors and lipids respectively and 2 accounts for the transmembrane nature of the receptors. Due to the lipid bilayer N_{lipids} is given by twice the liposome surface area ($A_{liposome}$) divided by the lipid headgroup area ($A_{lipid} = 0.67$ nm^2)[8].

Rewriting X_p (eq. 15) in terms of reduced densities yields

Eq. 16
$$X_P = \frac{\left(\dfrac{R_0^2}{A_{liposome}}\right)(N_{acceptor} + N_{donor})}{\left(\dfrac{R_0^2}{A_{liposome}}\right)(N_{acceptor} + N_{donor}) + \left(\dfrac{R_0^2}{A_{liposome}}\right)\dfrac{A_{liposome}}{A_{lipid}}} = \frac{(C_a + C_d)}{(C_a + C_d) + \dfrac{R_0^2}{A_{lipid}}} = \frac{C_t}{C_t + \dfrac{R_0^2}{A_{lipid}}}$$

Combining Eq. 11, 14 and 16 we can express E_{FRET} as a function of C_a, C_t, E_{bound} and K_a. In a weighted fit we could therefore extract E_{bound} and K_a when evaluating E_{FRET} as a function of C_a and C_t (**Fig. 3c**). K_a is used evaluate the standard Gibbs free energy change through eq. 13 applying T = 293.15 ± 14 Kelvin.

Supplementary Discussion

Discussion on proteoliposome formation and sample heterogeneities

Reconstitution of transmembrane proteins involves co-solubilization of receptors and lipids in detergent followed by removal of detergent either by rapid dilution, dialysis, gel chromatography or hydrophobic adsorption[9,10]. In the case where the proteoliposome formation process reaches a thermodynamic equilibrium, and no cooperative effects from lipids and partitioning proteins are present, we would expect a Poissonian distribution of empty and filled proteoliposomes when approaching a regime of low protein to lipid ratios. However this is not what we observe, which could suggest that the proteoliposome formation process is not at equilibrium but rather governed by kinetics, as previously suggested[11], or that cooperative processes are present. Oligomerization of incorporated proteins could constitute a cooperative factor. On the other hand heterogeneous distributions and in-efficient incorporation has been reported also for monomeric transmembrane proteins[12]. In general two main models explaining the mechanism of proteoliposome formation have been proposed[10,13,14].

Mechanism I: Protein incorporation and vesicle formation are two separate events. Detergent removal leads to the formation of separate lipid-protein-detergent and

detergent-lipid micelle species. Liposomes are formed from the detergent-lipid species, and protein inserts into these pre-formed detergent doped liposomes.

Mechanism II: The protein participates in the liposome formation process, where detergent removal results in constant coalescence between mixed micellar species.

In summary, proteoliposome formation is a complex process that is not well understood to date. The lack of techniques capable of monitoring and resolving in real time the molecular scale details of the inherently unstable protein/lipid/detergent structures renders the experimental insight to the mechanisms behind proteoliposome formation highly challenging. Resent progress[11,15] point towards the importance of changes in lipid collective properties upon addition of transmembrane proteins, suggesting a possible synergy between lipid and protein heterogeneities[16]. One way to gain further insight into the mechanism of proteoliposome formation would be to use single-particle fluorescence microscopy to monitor in real time their assembly during detergent dilution.

Discussion of obtained association constant

The reported energy gain for β_2AR association is about a factor of 2 higher compared to that of a single model transmembrane helix in DOPC lipid membranes[7], corresponding to a substantially (~17 fold) increased K_a. The fit yielded K_a in molefraction units, which allowed a direct conversion to association free energies. We converted to the corresponding dissociation constant in units of copies/area following the scheme published by Provasi *et al.*[6,17], yielding a K_d of 517 copies/μm^2.

β_2AR densities in the plasma membrane are generally in the range of 4-20 receptors per μm^2, depending on the cell type[18,19]. In addition, several reports indicate partial localization of β_2AR to membrane micro- or nano-domains where local densities

5

would be further enriched[20]. Based on our measurements (K_d of 517 copies/μm^2) one would estimate that β_2AR exist as a mixture of both monomers and dimers in living cells, which is consistent with data from single molecule tracking[21].

6

Supplementary note references

1.   Domanov, Y.A.*, et al. P Natl Acad Sci USA* **108**, 12605-12610 (2011).
2.   Wolber, P.K. & Hudson, B.S. *Biophys J* **28**, 197-210 (1979).
3.   Mansoor, S.E., Palczewski, K. & Farrens, D.L. *P Natl Acad Sci USA* **103**, 3060-3065 (2006).
4.   Kenworthy, A.K. & Edidin, M. *J Cell Biol* **142**, 69-84 (1998).
5.   Adair, B.D. & Engelman, D.M. *Biochemistry* **33**, 5539-5544 (1994).
6.   Fleming, K.G. *J Mol Biol* **323**, 563-571 (2002).
7.   Yano, Y. & Matsuzaki, K. *Biochemistry* **45**, 3370-3378 (2006).
8.   Marrink, S.J., de Vries, A.H. & Mark, A.E. *Journal of Physical Chemistry B* **108**, 750-760 (2004).
9.   Seddon, A.M., Curnow, P. & Booth, P.J. *Biochimica et Biophysica Acta (BBA) - Biomembranes* **1666**, 105-117 (2004).
10.   Rigaud, J.L., Levy, D., Mosser, G. & Lambert, O. *Eur Biophys J Biophy* **27**, 305-319 (1998).
11.   Jahnke, N.*, et al. Analytical Chemistry* **86**, 920-927 (2014).
12.   Heegaard, C.W., le Maire, M., Gulik-Krzywicki, T. & Moller, J.V. *J Biol Chem* **265**, 12020-12028 (1990).
13.   Rigaud, J.L. & Levy, D. *Liposomes, Pt B* **372**, 65-86 (2003).
14.   Helenius, A., Sarvas, M. & Simons, K. *Eur J Biochem* **116**, 27-35 (1981).
15.   Simeonov, P., Werner, S., Haupt, C., Tanabe, M. & Bacia, K. *Biophysical Chemistry* **184**, 37-43 (2013).
16.   Larsen, J., Hatzakis, N.S. & Stamou, D. *J Am Chem Soc* **133**, 10685-10687 (2011).
17.   Provasi, D., Johnston, J.M. & Filizola, M. *Biochemistry* **49**, 6771-6776 (2010).
18.   Mercier, J.F., Salahpour, A., Angers, S., Breit, A. & Bouvier, M. *J Biol Chem* **277**, 44925-44931 (2002).
19.   Hegener, O.*, et al. Biochemistry* **43**, 6190-6199 (2004).
20.   Patel, H.H., Murray, F. & Insel, P.A. G-Protein-Coupled Receptor-Signaling Components in Membrane Raft and Caveolae Microdomains. in *Protein-Protein Interactions as New Drug Targets*, Vol. 186 (eds. Klussmann, E. & Scott, J.) 167-184 (Springer Berlin Heidelberg, 2008).
21.   Calebiro, D.*, et al. Proc Natl Acad Sci U S A* **110**, 743-748 (2013).

7